Acta Oncologica, 2009; 48: 1181–1192

informa
healthcare

ORIGINAL ARTICLE

Dose prescription and optimisation based on tumour hypoxia

IULIANA TOMA-DAŞU[1], ALEXANDRU DAŞU[2] & ANDERS BRAHME[1]

[1]*Medical Radiation Physics, Stockholm University and Karolinska Institutet, 171 76 Stockholm, Sweden and* [2]*Radiation Physics, Department of Radiation Sciences, Umeå University, 901 87 Umeå, Sweden*

Abstract

Introduction. Tumour hypoxia is an important factor that confers radioresistance to the affected cells and could thus decrease the tumour response to radiotherapy. The development of advanced imaging methods that quantify both the extent and the spatial distribution of the hypoxic regions has created the premises to devise therapies that target the hypoxic regions in the tumour. *Materials and methods.* The present study proposes an original method to prescribe objectively dose distributions that focus the radiation dose to the radioresistant tumour regions and could therefore spare adjacent normal tissues. The effectiveness of the method was tested for clinically relevant simulations of tumour hypoxia that take into consideration dynamics and heterogeneity of oxygenation. *Results and discussion.* The results have shown that highly heterogeneous dose distributions may lead to significant improvements of the outcome only for static oxygenations. In contrast, the proposed method that involves the segmentation of the dose distributions and the optimisation of the dose prescribed to each segment to account for local heterogeneity may lead to significantly improved local control for clinically-relevant patterns of oxygenation. The clinical applicability of the method is warranted by its relatively easy adaptation to functional imaging of tumour hypoxia obtained with markers with known uptake properties.

Key Words: *Tumour oxygenation, vasculature, oxygenation, PET imaging, treatment optimization*

Tumour hypoxia is one of the main microenvironmental factors that modulate the response to radiotherapy through the resistance it confers to the affected cells and the promotion of their malignant development [1–6]. The radioresistance induced by the absence of oxygen at cellular level means that affected cells have to be irradiated with doses 2–3 times larger than the doses required to inactivate well oxygenated cells in order to obtain the same effect [7]. Consequently, at conventional dose levels the hypoxic radioresistance increases the probability that affected cells would survive radiotherapy and would subsequently repopulate the tumour and even lead to distant metastases. This could therefore explain the correlations between tumour hypoxia and poor clinical outcome. Several methods were consequently proposed to counteract the effect of hypoxic radioresistance ranging from increased use of oxygen [8–10] or administering oxygen-mimetic radiosensitisers [11–13] to using different radiation qualities [14,15] or escalating the dose administered with conventional radiation qualities [16]. However, the success of the strategies aimed to counteract the effects of tumour hypoxia depends on the availability of accurate information about the tumour oxygenation status at various points during the treatment.

Several methods are now available to quantify tumour oxygenation or hypoxia as recently reviewed by Daşu and Toma-Daşu [17] or Krohn et al. [18] and the results are usually used for predictive purposes or for selecting patients for dedicated treatment approaches. However, the most promising methods for an effective optimisation of the treatment are the imaging techniques that can provide information on the severity as well as on the spatial distribution of the hypoxic areas. Indeed, it has been suggested by Ling et al. [19] that imaging information could be used to define a biological target volume besides the conventional target volumes that may improve target delineation and dose delivery. The results of modelling studies like that of Tome and Fowler [20] also suggested that selectively boosting the dose to a small tumour subvolume could lead to improved local control. Subsequent modelling studies presented

Correspondence: Iuliana Daşu, Medical Radiation Physics, Karolinska Institutet, 17176 Stockholm, Sweden. Tel: +46 8 51774839. Fax: +46 8 343525. E-mail: iuliana.livia.dasu@ki.se

(Received 13 February 2009; accepted 12 July 2009)

ISSN 0284-186X print/ISSN 1651-226X online
DOI: 10.3109/02841860903188643

several approaches with various degrees of complexity that have been proposed for the inclusion of imaging information into treatment planning. One of the most common methods is to delineate a hypoxic subtarget in the tumour to which to prescribe a more or less empirical escalation of the dose according to the available radiation therapy technique and the tolerance of the normal tissues around the tumour [21–23]. The risk however is that the prescribed dose is not large enough to counteract the hypoxic radioresistance and therefore the method might fail to bring the expected results in a clinical setting. Other approaches recommended highly heterogeneous dose distributions based on a linear increase of the prescribed dose according to the signal intensity in positron emission tomography (PET) or magnetic resonance (MR) images [24–26] or as a result of redistributing the dose to the target by increasing the dose to the hypoxic voxels while decreasing the prescribed dose to the remaining voxels in the tumour [27–29]. Heteorgeneous dose distributions however are at risk of failing to provide expected results for cases of dynamic hypoxia as have indeed been seen in clinical patients [30,31]. More complex approaches for heterogeneous dose prescription make use of dynamic PET information [32] or the adaptation of the prescribed doses based on two successive PET images taken during the treatment [33].

A potentially weak aspect of the proposed approaches is the issue of dose prescription. Thus, empirical dose prescriptions might not result in doses that are large enough to counteract the hypoxic radioresistance and therefore the methods employing them are at risk of leading to disappointing results in a clinical setting. Similarly, the dynamics of the highly heterogeneous hypoxic regions could change the spatial distribution of hypoxia and this could easily lead to mismatches between the hypoxic subregions and the planned hotspots in the distribution. This study aims to address these issues and proposes a novel method for objective dose prescription taking into account both the extent and the heterogeneity of hypoxia. The principle of the method could however be used for any imaging technique and any physiological aspect that is known to influence the response to radiation therapy.

Materials and methods

Dose prescription and optimisation

An objective method for dose prescription could be derived from the cellular response to radiation. Thus, the starting point is the spatial distribution of cellular density, $n(\mathbf{r})$ after a dose distribution $D(\mathbf{r})$ that is given by Equation 1.

$$n(\mathbf{r}) = n_0(\mathbf{r}) \cdot s(\mathbf{r}) \tag{1}$$

where $n_0(\mathbf{r})$ is the initial cell density distribution and $s(\mathbf{r})$ is the spatial distribution of the cell survival as a function of the local dose $D(\mathbf{r})$ and the local radiosensitivity.

The surviving fraction of cells $s(\mathbf{r})$ could be calculated with various biological models. The most widely used model to describe the response of cells and tissues to fractionated treatments with nonuniform doses per fraction is the LQ model [34–36] in Equation 2.

$$s[d(\mathbf{r}), \alpha(\mathbf{r}), \beta(\mathbf{r})] = [\exp(-\alpha(\mathbf{r}) \cdot d(\mathbf{r}) - \beta(\mathbf{r}) \cdot d^2(\mathbf{r}))]^n \tag{2}$$

where n is the number of fractions, $d(\mathbf{r})$ is the dose per fraction and $\alpha(\mathbf{r})$ and $\beta(\mathbf{r})$ are the radiosensitivity parameters modified according to the local oxygen tension through the oxygen enhancement ratio (OER) proposed by Alper and Howard-Flanders [37].

$$OER = \frac{OER_{\max}(k + pO_2)}{k + OER_{\max}\, pO_2} \tag{3}$$

where OER_{max} is the maximum effect that is achieved in the absence of oxygen, k is a reaction constant and pO_2 is the local oxygen tension. Biologically relevant values were used for the parameters in Equation 3 ($OER_{max} = 3$, $k = 2.5$ *mmHg*) [7,38].

For the purpose of illustrating the formalism proposed in this paper and to describe the clinically expected tumour response, the parameters in Equation 2 were assumed to give a cell survival fraction of 0.5 at 2 Gy (SF_2) with $\alpha/\beta = 10$ Gy ($\alpha = 0.29$ Gy^{-1}) for the fully oxygenated tumour cells [39]. It was further assumed that the total cell population at the beginning of the treatment was 10^8 cells. This set of parameters is thought to be applicable for many tumours treated with doses in the clinical range. For particular clinical applications however special sets of LQ parameters could be easily derived from clinical dose response curves as proposed by Ågren-Cronqvist et al. [40].

The relationship between cell survival and tumour response expressed as the local tumour control probability, P, is described by the Poisson expression in Equation 4 as the result of integrating the density of the surviving cells in Equation 1 over the whole tumour volume.

$$P = e^{-\overline{N}} = \exp\left\{-\int_{\mathbf{r}} n_0(\mathbf{r}) \cdot s(\mathbf{r}) d\mathbf{r}\right\} \tag{4}$$

For the case of tumours composed of individual voxels, as generally available from modern imaging methods, the integral in Equation 4 transforms into a summation over all the constituent voxels in the tumour with volumes V_j, as in Equation 5.

$$P = e^{-\overline{N}} = \exp\left\{-\sum_{V_j} n_0(V_j)\cdot s(V_j)\cdot V_j\right\} \qquad (5)$$

It should be noted that the expression in Equation 5 is quite general as it does not impose any limitations with respect to the size or the shape of the tumour.

This expression, in combination with Equations 1–3 above could be used to calculate the doses needed to ensure a local control P. Thus, assuming that at the end of the treatment the cellular density should be uniform throughout the tumour and equal to $n(\mathbf{r}) = \dfrac{-\ln(P)}{V}$, with V the tumour volume [41], a dose distribution that would lead to a level of tumour control P is given by Equation 6.

$$\hat{D}(\mathbf{r}) = n\frac{\alpha(\mathbf{r})}{2\beta(\mathbf{r})}\left[\sqrt{1+\frac{1}{n}\frac{4\beta(\mathbf{r})}{\alpha^2(\mathbf{r})}\ln\left(\frac{Vn_0(\mathbf{r})}{-\ln P}\right)}-1\right] \qquad (6)$$

Equation 6 is a general expression that could be used for any initial distribution of cell density, $n_0(\mathbf{r})$, within the tumour volume V and for any functions $\alpha(\mathbf{r})$ and $\beta(\mathbf{r})$ describing the cellular radiosensitivity.

The dose distribution $\hat{D}(\mathbf{r})$ as predicted by Equation 6 may be highly heterogeneous as it has to account for the variability in radiosensitivities given by the variations in the local oxygenation of the tumour. Indeed tumour oxygenation is characterised by considerable heterogeneity given by the steep gradients that characterise the oxygen diffusion into the tissue as it has been shown both in experimental observations [42] and in theoretical simulations [43,44]. In general, highly heterogeneous dose distributions are quite difficult to deliver with usual techniques. Furthermore, it is known that the cellular pO_2 changes during the course of fractionated radiotherapy and that this change could lead to temporal variations of the radiosensitivity at the voxel level. Such variations have indeed been observed in clinical studies that used multiple imaging of tumours during the treatment duration [30,31]. Thus, all these variations may lead to a loss in the tumour control from the preset level when the local oxygenation changes while the same heterogeneous dose distribution is delivered at every fraction. This happens because the overdosage of a radiosensitive region could not account for the underdosage of a radioresistant region due to the non-linear relationship between cell survival and dose.

The simplest method to account for these variations would be to deliver a rather high uniform dose to the whole tumour that accounts for the maximum hypoxic protection that may be encountered. However, such an approach may not be feasible in the light of the toleration limitations of the normal tissues nearby. A more robust solution to overcome this limitation is to simplify the dose distribution by segmenting the target volume into several regions according to the regional distribution of radiosensitivities and delivering a homogeneous dose to each region. This approach would however require a robust method to prescribe the dose to each segment taking into consideration the local heterogeneity in radiosensitivity.

It has previously been shown that for a tumour with homogeneous radiosensitivity a heterogeneous dose distribution will lead to a decrease of the control probability due to the non-linear relationship between radioresistance, dose and cell survival [45]. However this observation is also relevant for dynamic variations of the heterogeneity in the considered target volume if one can assume that the overall average radiosensitivity is constant and the temporal variations take place around a mean value. Indeed, in this case the product of individual survival over several fractions would be given mainly by the average radiosensitivity. Hence, one could assume in turn that the loss of the tumour control probability would be the effect of dose heterogeneity in the target. The magnitude of this effect could be quantified by taking into account the mathematical expansion of the tumour control probability as a function of dose (Equation 7).

$$P(D(\mathbf{r})) = P(\overline{D}) + \frac{D^2(\mathbf{r})}{2}\frac{\partial^2 P}{\partial D^2}\left(\frac{\sigma_D}{D(\mathbf{r})}\right)^2 + \ldots \qquad (7)$$

where $D(\mathbf{r})$ is a heterogeneous dose distribution with average $\overline{D}$ and standard deviation σ_D.

The expression in Equation 7 might be interpreted to suggest that variations in tumour control probability are given by the heterogeneity in the delivered dose distribution. However, it should be noted that for the case under discussion, Equation 7 reflects the effects of the heterogeneity of the planned dose distribution that results from the individual radiosensitivities according to Equation 6. It can nevertheless be seen that the effect of a uniform dose equal to the mean of the distribution differs from the effect of the heterogeneous dose distribution. This is because the increased survival in the low dose areas is not compensated by the decreased survival in the high dose areas. It has also been shown [45,46] that the response of the tumour to a heterogeneous dose distribution will correspond to a homogeneously distributed effective dose that is lower than the average delivered dose (Equation 8).

$$D_{eff} = \overline{D}\left[1-\frac{\gamma}{2P(\overline{D})}\left(\frac{\sigma_D}{\overline{D}}\right)^2\right] \qquad (8)$$

where $\overline{D}$ is the average of the dose distribution, in the present case $\hat{D}(\mathbf{r})$, γ is the normalised slope of the dose response curve of the tumour and σ_D^2 is the variance of the heterogeneous dose distribution,

$\hat{D}(\mathbf{r})$. The value used for simulations ($\gamma = 4$) is representative for many human tumours [46].

Thus, it appears that in order to avoid the predicted loss of control due to heterogeneity, the doses to each segment have to be adjusted to ensure close to uniform tumour effect. From Equation 8 it results that a prescribed uniform dose, D_P, which could counteract the effects of dose heterogeneity in each segment ensuring a level of tumour control probability P would be given by the expression in Equation 9.

$$D_P = \frac{\overline{D}}{\left[1 - \frac{\gamma}{2P(\overline{D})}\left(\frac{\sigma_D}{\overline{D}}\right)^2\right]} \tag{9}$$

In the clinical setting the distribution of radiosensitivities would have to be determined from imaging methods. It should however be stressed that the formalism proposed above is not limited to any particular imaging method. It provides a universal and simple method to account for the effects of the heterogeneity in radiosensitivity in the target measured with any method.

Investigating the efficiency of the proposed method for dynamic hypoxia

Clinical and experimental tumours generally have heterogeneous oxygenations resulting from poor vascular structures, acute hypoxia and low oxygen content of the individual blood vessels that usually originate from the venous vasculature [47]. Thus, tumour hypoxia appears due to diffusion limitations in regions far from active blood vessels or around temporarily non-perfused blood vessels. These different causes lead to considerable heterogeneity of the tumour oxygenation with respect to the spatial distribution [42,43]. Furthermore, increased proliferation and angiogenesis in tumours may also lead to dynamic changes of the pattern of oxygenation. There is therefore the risk that mismatches between radioresistent regions and planned hotspots in the dose distributions would lead to loss of local control. The magnitude of this loss could in principle be determined in clinical studies employing a sufficiently large patient population. However, such a study would be rather difficult to implement in practice, both due to ethical and logistic issues. An alternative would be to investigate the effectiveness of the method though theoretical simulations.

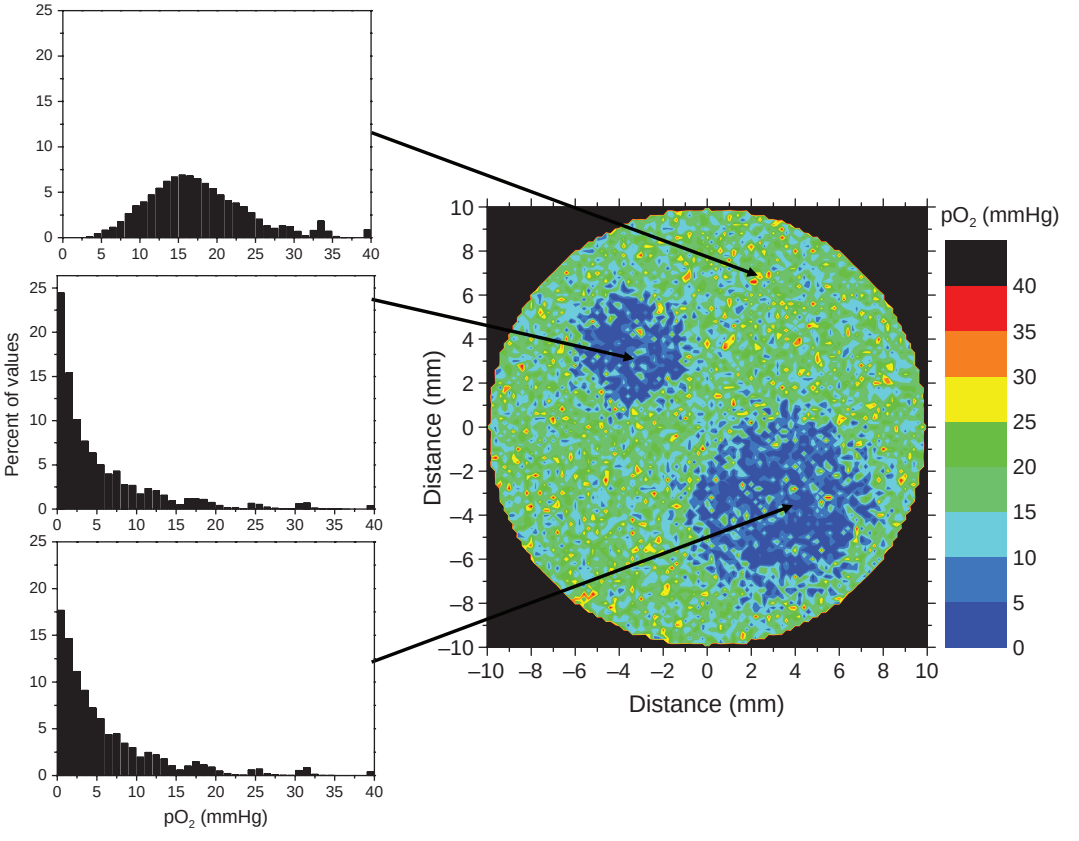

Figure 1. Simulated oxygen distribution in a theoretical tumour used in this study. It was assumed that the simulated tumour has two hypoxic islands surrounded by cells that are better oxygenated. The local oxygen distributions for each region are indicated in the insets.

Theoretical modelling is a reliable method capable of simulating the effects of radiation therapy and providing a quick estimation of various treatment gains or losses before lengthy and expensive clinical trials are set up. Results from previous simulations of tissue oxygenations [17,43,48,49] have been used as input for a Monte-Carlo algorithm to generate theoretical three-dimensional tumours with different morphological sub-regions similar to those imaged in patients. Figure 1 shows an example of oxygen distribution in a section through a simulated tumour. The influence of the dynamics of oxygenation throughout the treatment was investigated by modifying the oxygen distributions in the tumours and thus simulating possible inter-fractional changes of tumour oxygenation that may occur in fractionated treatments. Different patterns and frequencies of changes in oxygenation were taken into consideration as illustrated in Figure 2. Thus, it was first assumed that the reoxygenation could only affect the distribution at the microscopic level, while the overall regional oxygenations remain the same. This pattern is thought to give the influence of the dynamic changes of acute hypoxia that result on the microscopic level from the closure and opening of blood vessels in the tumour. Another pattern of oxygenation assumed that the hypoxic islands in the tumour could shrink during the course of the treatment. This

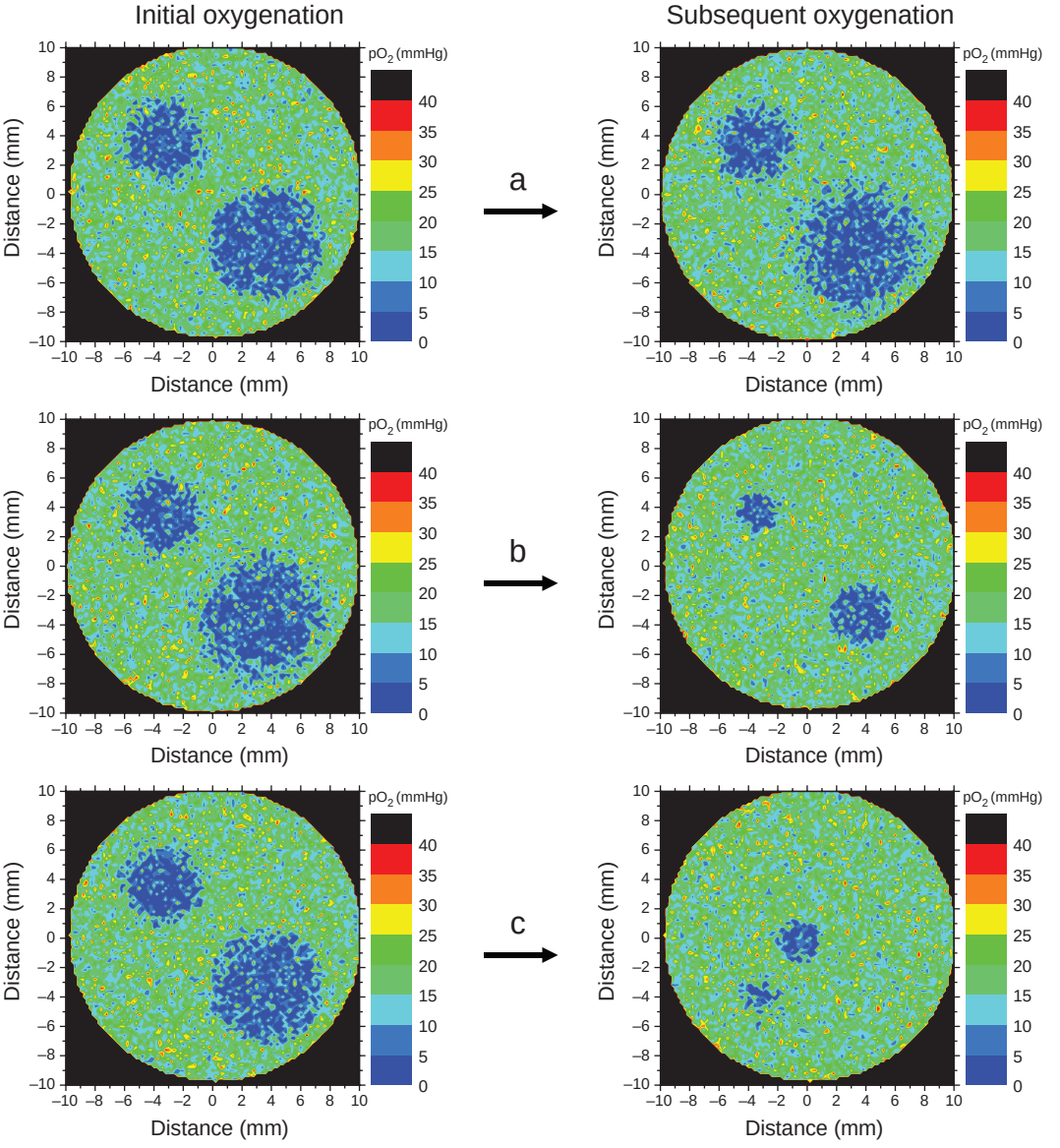

Figure 2. Different patterns of oxygenation simulated in the study. (a) The reoxygenation affects the distribution at the microscopic level only, while the overall regional oxygenations remain the same. (b) The hypoxic islands in the tumour shrink during the course of the treatment. (c) The regional oxygenations might change location due to complex patterns of vascular failure that may occur during the treatment.

could be regarded as modelling the shrinkage of the chronic hypoxic compartment as the result of the overall improvement of oxygenation. Yet, a third pattern of changes in oxygenation took into account the possibility that the hypoxic regions might change location due to more complex patterns of vascular failure that may occur during the treatment. Similar dynamic patterns were indeed observed in clinical patients [30,31] when repeated PET investigations were performed during the course of the treatment. Different reoxygenation patterns were taken into consideration when studying the influence of hypoxia dynamics, from no change of the oxygenation during the whole treatment up to changes at every delivered fraction. Several degrees of shrinkage of the hypoxic subregions were therefore modelled, e.g., 20%, 30%, 60%, 80% etc. This covers all the possible reoxygenation rates that may be encountered in clinical tumours, from the rapid reoxygenation of acute hypoxia characterised by timescales of a few minutes or hours to the slow reoxygenation brought about by the removal of the inactivated cells and which may have a timescale extending over several days or weeks.

Oxygenation maps like the one in Figure 1 were used as a starting point to calculate dose distributions that will give a tumour control of 90% under the assumption that the radiosensitivity distribution given by hypoxia remains unchanged throughout the treatment. The first step was the transformation of the oxygenation maps into distributions of radiosensitivities with the help of Equation 3. These were subsequently used in Equation 6 to calculate the heterogeneous dose distribution required to achieve the predefined tumour control probability. Segmented dose distributions were also calculated for the hypoxic regions according to Equation 9. The resultant dose distributions were then used to calculate the influence of various patterns of reoxygenation in the tumours. The results of the analysis were quantified in terms of the tumour control probability according to Equation 5.

Results

Figure 1 shows a realistic tumour oxygen distribution generated according to the principles described in the section on Materials and methods. It was assumed that the tumour has two hypoxic subvolumes surrounded by cells that are better oxygenated, but not as well as the normal tissues. The local oxygen distributions for each region are indicated in the insets. For simplicity, a spherical shape was assumed in this study both for the tumours and their subregions, but this has little implications on the algorithm used to calculate optimum dose distributions as it operates on a voxel basis for which the shape of the target is irrelevant.

The resultant dose distributions for the tumour oxygenation in Figure 1 are presented in Figure 3. Thus, panel 3a shows the heterogeneous dose distribution required according to Equation 6 to achieve the predefined tumour control probability (average dose $\pm$ standard deviation: 68 $\pm$ 11 Gy), while panel 3b shows the segmented dose distribution calculated for each subregion according to Equation 9 resulting in prescribed doses of 68 Gy (regional average dose $\pm$ standard deviation: 67 $\pm$ 6 Gy), 103 Gy (86 $\pm$ 23 Gy) and 110 Gy (90 $\pm$ 26 Gy). The resultant dose distribution in Figure 3b has the advantage that it could be relatively easily delivered in clinical practice with existing techniques comparatively to the highly heterogeneous distribution in Figure 3a. As described in the section on Materials and methods, the dose distributions in Figure 3 were used to calculate the expected tumour control probabilities for various

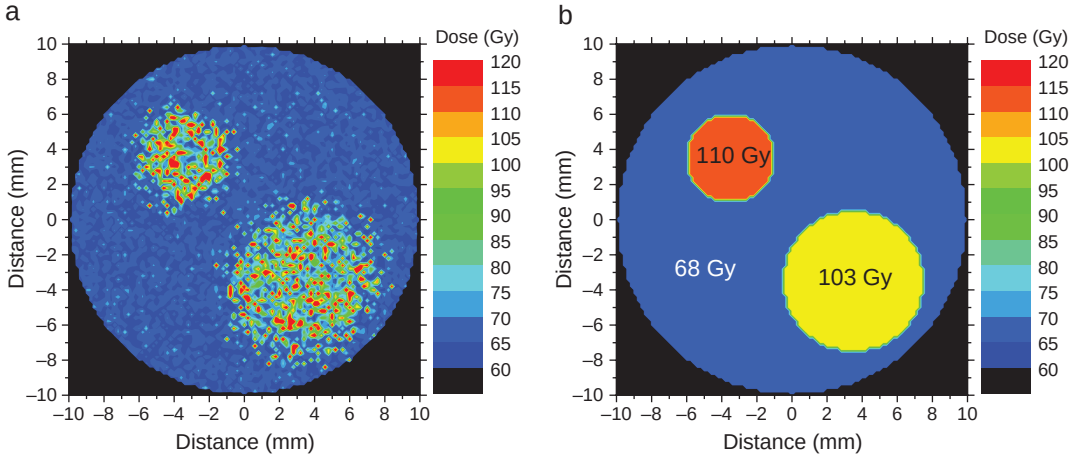

Figure 3. Dose distributions calculated to give a predefined tumour control level of 90%; (a) – heterogeneous distribution, $\hat{D}(\mathbf{r})$, calculated with Equation 6 from the derived radioresistance map of the tumour; (b) – segmented dose distribution, D_P, calculated with Equation 9.

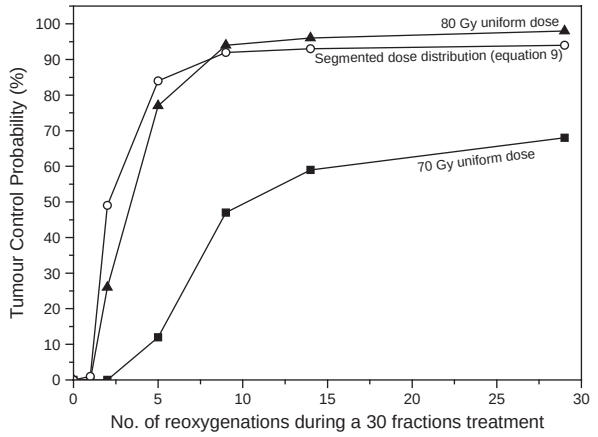

Figure 4. Variations in the achievable tumour control probability due to modifications of the hypoxic pattern in the tumour. Solid symbols show the response to uniform doses delivered to the target. Open symbols show the response to a segmented dose distribution derived with Equation 9.

patterns of reoxygenation in the tumours. Comparisons were performed with the predicted results from irradiating the tumour with uniform doses that could be used in clinical practice. The results are summarised in Figure 4 and Table I.

As expected, assuming that the hypoxic regions remain completely unchanged throughout the treatment, the resultant tumour control was practically zero when uniform or segmented dose distributions were delivered to the tumour. The explanation is that for static populations the response to radiation is totally governed by the very radioresistant initial hypoxic compartment and that the relatively modest dose increases that may be achieved in the clinic for uniform irradiation are most likely insufficient to counteract the radioresistance of the hypoxic cells that require doses 2–3 times higher than the well oxygenated tumour cells. This situation however is seldom encountered in the clinic where the relatively high cure rates observed indicate quite strongly that reoxygenation does indeed take place during the treatment and that the oxygenation compartments are not static [7]. Various reoxygenation patterns were indeed observed in clinical tumours investigated repeatedly during radiation therapy with F-MISO PET [30,31].

Probably the most encountered pattern of reoxygenation in clinical and experimental tumours is given by the behaviour of acute hypoxia caused by the temporary closure and opening of the blood vessels which determine the oxygenation dynamics on the microscopic level. Figure 4 shows that when it was assumed that individual voxels could have acutely

Table I. Predicted tumour control probabilities for various numbers of reoxygenations.

	Tumour control probability (%)					
			Uniform dose distribution with the specified value			
Number of reoxygenations	Heterogeneous dose distribution	Segmented dose distribution	**60 Gy**	**70 Gy**	**80 Gy**	**90 Gy**
Reoxygenation of acute hypoxia						
0	90	0	0	0	0	0
1	55	1	0	0	0	27
2	46	49	0	0	26	77
4	50	84	0	12	77	97
9	57	92	0	47	94	99
14	60	93	0	59	96	100
29	63	94	0	68	98	100
Reoxygenation of acute and chronic hypoxia						
0	90	0	0	0	0	0
1	62	5	0	0	1	30
2	58	75	0	0	34	82
4	67	94	0	26	85	98
9	80	95	2	76	98	100
14	84	95	12	89	99	100
29	87	96	34	97	100	100
Complex reoxygenation patterns						
0	90	0	0	0	0	0
1	59	11	0	0	3	44
2	69	48	0	56	94	99
4	82	90	16	93	100	100
9	85	94	29	96	100	100
14	86	95	35	97	100	100
29	87	95	39	98	100	100

varying oxygenations throughout the treatment while the overall regional oxygenation of the tumour remains in agreement with the distributions used as input, the control improves considerably both for uniform doses and for the segmented dose distributions targeting the hypoxic regions when the reoxygenation rate increases to the levels that are considered relevant for real tumours (above 4 or 5 reoxygenations which would correspond to weekly changes or even faster). In these conditions it is quite likely that microscopic hypoxic regions at a certain moment could also be irradiated in a better oxygenated state and therefore be effectively sterilised, resulting in an increased tumour control probability. At the same time, the effectiveness of the highly heterogeneous dose distributions decreases as a result of the mismatches on voxel-level between hypoxic regions and planned dose hotspots.

Furthermore, for uniform irradiation of the whole tumour, one needs a considerable increase of the dose, above 80 Gy, to achieve improved control. This dose might not be delivered in most cases due to the limitations imposed by the tolerance of the healthy organs nearby. However, targeting the hypoxic regions in the tumour with a segmented distribution with doses that take into account the oxygenation heterogeneity according to Equation 9 could result in similar levels of control for a lower average dose to the tumour or a lower dose to the outer rim of the tumour tissue. Such a dose distribution could also be achieved with a decreased dose burden to the sensitive normal tissues near the tumour and could hence result in reduced complication rates.

The mid-section in Table I shows the effects of another pattern of hypoxia dynamics that accounts for the relative shrinkage of the hypoxic regions in the tumour. Indeed, it has been observed that as the treatment progresses the overall oxygenation of a tumour could improve as a result of the improved vascular flow and the reduction of the bulk tumour volume. The response pattern of a heterogeneous dose distribution and the segmented dose distributions is similar to those for acute reoxygenation. Furthermore, the tumour response for the segmented dose distribution improves rapidly for dynamic tumours and high tumour control levels are more easily achieved as the hypoxic fraction decreases throughout the treatment and the remaining oxic population is comparatively more effectively sterilised. The overall pattern is maintained even when changes in location within the tumour accompany the shrinkage of the hypoxic regions as shown in the last section of Table I. The control levels at the end of the treatment are somewhat lower for migrating hypoxic regions, as the high dose regions would no longer match the intended targets, but the impact appears rather small when the overall oxygenation of the tumour improves. However, in this case highly heterogeneous dose distributions could also lead easily to regional dose mismatches that would consequently result in a more pronounced decreased probability to control the tumour. The results therefore highlight the advantages of using a segmentation of complex dose distributions according to the algorithm proposed in this study that not only delivers a more manageable dose distribution, but could also account for changes in the hypoxic pattern determined by the microscopic fluctuations of acute hypoxia.

These results also show that the efficiency of the individualization of the treatment plans based on imaging tumour hypoxia depends on the approach used to prescribe the doses to the target. Thus, neglecting the effects of dynamic hypoxia could lead to considerable loss of control for highly heterogeneous dose distributions due to mismatches between planned dosimetric hotspots and hypoxic regions. In contrast, optimised dose distributions preferably based on the segmentation of the hypoxia images and prescribing the dose to account for local heterogeneity as proposed in this study could indeed result in improved local control.

Discussion

Tumour hypoxia is an important microenvironmental factor that confers resistance to radiotherapy [50]. The hypoxic environment may also generate a more aggressive malignant phenotype, thus increasing the risk for distant metastases. These observations have identified tumour hypoxia as one of the most important therapeutic problems for cancer treatment. A recent analysis of clinical data has shown that a significant fraction of the patients are adversely affected by hypoxia and could therefore benefit from dedicated treatment approaches intended to counteract its effects [51].

The development of advanced imaging methods capable of quantifying the extent and the spatial distribution of the hypoxic regions has opened new possibilities for anti-hypoxic therapies. Thus one could use diagnostic images to define physiological target volumes and to devise advanced treatment plans depending on their expected responsiveness. Several methods were proposed towards this aim and their feasibility was investigated in theoretical planning studies [21–29]. However, their efficiency to achieve improved local control in patients has not been investigated in clinical studies, one major concern being the possibility of mismatches between hypoxic areas and planned dose escalations caused by

the temporal variation of hypoxia. It is therefore only through theoretical simulations that the efficiency of any such method can be evaluated. The success of the simulation of course depends on how well it can mimic the different aspects that have been observed in reality.

This study presented an original method to prescribe dose distributions that focus the radiation dose to the radioresistant regions and spare adjacent normal tissues. The efficiency of the method has been tested in clinically-relevant simulations of tumour hypoxia. Careful steps were taken to include several aspects that may appear for clinical tumours. Thus, it was assumed that oxygenation is heterogeneously distributed throughout the tumour and that different tumour regions could have different oxygenations that may change during the treatment duration as has been observed in clinical patients [30,31]. Under these conditions it has been shown that tumour hypoxia dynamics in general and the reoxygenation rates in particular can influence the success of various optimization approaches. Highly heterogeneous dose distributions may lead to significant improvements of the outcome only for static oxygenations. In contrast dynamic hypoxia could significantly reduce their effectiveness when the complex dose distributions mismatch the hypoxic regions. This has indeed been a matter of concern for strategies devised only on pre-treatment investigations that do not take into consideration the evolution during therapy [25]. However, segmenting the dose distributions and optimising the dose prescribed to each segment to account for local heterogeneity may be a solution to reduce the variability in regional mismatches and could therefore lead to improved local control. The results of the simulations have also shown that this method appears to lose effectiveness only when the oxygenation pattern changes less than three to four times throughout the whole treatment. These frequencies are highly unrealistic for conventional schedules as they imply that oxygenation changes only once every two or three weeks. Indeed, the known reoxygenation rates of acute hypoxia are of the order of a few minutes [52–54] and clinical observations of tumour oxygenation show that the hypoxic pattern could change significantly in weekly investigations [30,55]. Hence, for most clinical cases, the proposed method based on segmentation is thought to lead to an increased probability of cure while limiting the irradiation of the surrounding normal tissues. The present study also indicates that when hypofractionated stereotactic radiotherapy is used a significantly higher dose would be required due to lack of reoxygenation and severely radioresistant compartments. This applies at least when five or less fractions are being used. For more than five fractions, Equation 9 may be used to adjust for hypoxic radioresistance using segmented dose delivery as discussed above.

The practical implementation of the method on patient images deserves particular attention as direct information on the tumour oxygenation is needed. Such information could be obtained from PET imaging with dedicated tracers that are metabolised and trapped in the affected cells. Other imaging methods like perfusion studies with Blood Oxygen Level Dependant (BOLD) MRI provide information mainly on the tissue vasculature that is an indirect measure of the tissue oxygenation which is modulated by the vascular density of the tissue [17]. Alternative methods like the use of fluorocarbon reporter molecules are required to obtain direct indications of the tissue oxygenation.

Clinical PET investigations of tumour hypoxia could now be performed with several bioreductive markers that have selective retention in the hypoxic cells. Hypoxia imaging with nitroimidasole tracers for example is based on the competition of the compound with the intracellular oxygen and the accumulation of the former in cells in which the latter is in short supply [56]. In order to use clinically the formalism proposed above, the distribution of radiosensitivities could be obtained by converting the observed PET intensities using the binding characteristics of the tracer used giving the uptake in a known level of oxygenation. From this point of view, experimentally determined uptake curves for PET tracers have the potential to provide more accurate conversions of the image intensities into distributions of oxygenation and hence of radioresistance [57]. Experimental data on the relationships governing the uptake of the hypoxic tracers are relatively scarce [58,59] indicating the general interest directed mainly towards the qualitative evaluation of the PET images. However, the potential of tailoring radiation treatments could only be reached through the accurate quantification of the images when such relevant relationships become available since these relationships could be used to determine an objective correlation between the image intensities (given by the local uptake rates) and the local oxygenation. In practice, the uptake curves could be normalised to a level of oxygenation well defined or easily obtainable for a tissue (for example the oxygenation of a muscle or a well-vascularised organ that appears in the diagnostic image) similar to the usual normalisation of the PET images. This could therefore provide a method of quantifying the activities measured in PET images. The predicted distributions of local oxygenations could be further converted into distributions of radioresistances with the help of Equation 3, thus

obtaining an objective conversion of the intensities in the measured images into distributions of radioresistances, more accurate than empirical assumptions of the relationship between the two.

Several other aspects could influence the quantification of the tissue oxygenation and their impact has to be taken into consideration for any optimisation approach. Thus, a general matter of concern for the *in vivo* imaging of hypoxia is the ability of the tracer to reach the cells through the vascular network, bearing in mind that the same vascular network is responsible for the appearance of hypoxia in tumours. However, this is less of a problem for nitroimidasoles since it has been shown in many experiments that they could reliably image hypoxia appearing in animal and human tumours far from active blood vessels or around collapsed blood vessels [42,60]. Another potential problem is that tumours could be a mix of tumour and stroma cells that may have different uptake properties which could eventually influence the image intensities. However, the good correlations between PET hypoxia and results from other measurement methods [61,62] suggest that the impact of these aspects may not hamper the quantification of the PET images.

Another aspect that may influence the prescription of the dose and the efficiency of optimisation methods is the averaging over rather large tissue volumes that is characteristic to many imaging modalities. It has been shown that even for polarographic methods that average over relatively small tissue volumes the measured oxygenation could be quite different from the real tissue oxygenation and this may translate into different predictions regarding tissue responsiveness to radiation therapy [63,64]. This could be even more of a problem for present imaging techniques that provide average oxygenations which may underestimate the radioresistance of the microscopic hypoxic regions. Thus, the small hypoxic regions that may not be rendered effectively in the images could be underdosed even with voxel-defined heterogeneous dose distributions. This aspect is however expected to have less impact on methods taking into account the dynamic character of tumour hypoxia and thus minimising the mismatches between planned dosimetric hotspots and hypoxic regions. The limiting factor in this case could be the reduced heterogeneity of oxygenation that appears in the measurements and which influences the prescribed doses. The effectiveness of the method could however be improved if information on the oxygenation heterogeneity could be obtained from other means. This might be less of a problem in modern medical approaches that involve multiple tests before the treatment.

Improved results would be obtained if several other physiological factors that influence the treatment outcome are also taken into consideration. Algorithms have been proposed to include information regarding the local density of clonogenic cells and their proliferation rate [65] and they could be easily combined with the algorithms targeting tumour hypoxia. Further improvements of the cure rates could also be achieved by monitoring the tumour and adapting the treatment to the clinically observed variations in radiation responsiveness as proposed for example for the BIOART approach [33].

For the practical implementation of optimisation approaches targeting physiological factors with adverse effects on treatment outcome, special attention has to be paid to target movement and patient positioning. These are general issues of concern for all radiation treatment approaches, but they become increasingly important for treatments employing non-uniform dose distributions. The degree of accuracy needed of course decreases when the heterogeneity of the prescribed dose decreases as for segmented dose distributions. Nevertheless, in order to minimise the effects of target motion, modern treatment approaches require integration with methods to image the position of the target in relation to the beam location and the adjacent normal organs.

Conclusions

This study presents a robust method to prescribe minimum dose levels that are required to counteract various levels of hypoxic radioresistance in tumours. The proposed approach is thought to lead to improved local control as it takes into consideration aspects like hypoxia dynamics and heterogeneity that have been of concern for other dose prescription approaches. The simulations performed as part of the study have also highlighted the need to adapt the prescription approach to the radiation delivery method available. Thus, conventionally fractionated regiments will benefit from the use of segmented dose distributions with uniform doses per segments, while hypofractionated regiments employing less than about 5 fractions might benefit from the use of more heterogeneous dose distributions if they could be delivered in practice.

Acknowledgements

Financial support from Vinnova, 6th FP of EU and the Cancer Research Foundation in Northern Sweden is gratefully acknowledged.

Declaration of interest: There is no conflict on interests regarding this study.

References

[1] Höckel M, Knoop C, Schlenger K, Vorndran B, Baussmann E, Mitze M, et al. Intratumoral pO2 predicts survival in advanced cancer of the uterine cervix. Radiother Oncol 1993;26:45–50.

[2] Nordsmark M, Overgaard M, Overgaard J. Pretreatment oxygenation predicts radiation response in advanced squamous cell carcinoma of the head and neck. Radiother Oncol 1996;41:31–9.

[3] Brizel DM, Dodge RK, Clough RW, Dewhirst MW. Oxygenation of head and neck cancer: Changes during radiotherapy and impact on treatment outcome. Radiother Oncol 1999;53:113–7.

[4] Höckel M, Vaupel P. Biological consequences of tumor hypoxia. Semin Oncol 2001;28:36–41.

[5] Fyles A, Milosevic M, Hedley D, Pintilie M, Levin W, Manchul L, et al. Tumor hypoxia has independent predictor impact only in patients with node-negative cervix cancer. J Clin Oncol 2002;20:680–7.

[6] Carnell DM, Smith RE, Daley FM, Saunders MI, Bentzen SM, Hoskin PJ. An immunohistochemical assessment of hypoxia in prostate carcinoma using pimonidazole: Implications for radioresistance. Int J Radiat Oncol Biol Phys 2006; 65:91–9.

[7] Hall EJ, Giaccia AJ. Radiobiology for the radiologist, 6th ed. Philadelphia: Lippincott Williams & Wilkins; 2006.

[8] Watson ER, Halnan KE, Dische S, Saunders MI, Cade IS, McEwen JB, et al. Hyperbaric oxygen and radiotherapy: A Medical Research Council trial in carcinoma of the cervix. Br J Radiol 1978;51:879–87.

[9] Saunders MI, Hoskin PJ, Pigott K, Powell ME, Goodchild K, Dische S, et al. Accelerated radiotherapy, carbogen and nicotinamide (ARCON) in locally advanced head and neck cancer: A feasibility study. Radiother Oncol 1997;45: 159–66.

[10] Kaanders JH, Pop LA, Marres HA, Liefers J, van den Hoogen FJ, van Daal WA, et al. Accelerated radiotherapy with carbogen and nicotinamide (ARCON) for laryngeal cancer. Radiother Oncol 1998;48:115–22.

[11] Dische S. Chemical sensitizers for hypoxic cells: A decade of experience in clinical radiotherapy. Radiother Oncol 1985;3: 97–115.

[12] Overgaard J. Clinical evaluation of nitroimidazoles as modifiers of hypoxia in solid tumors. Oncol Res 1994;6: 509–18.

[13] Overgaard J, Horsman MR. Modification of Hypoxia-induced radioresistance in tumors by the use of oxygen and sensitizers. Semin Radiat Oncol 1996;6:10–21.

[14] Fowler JF. Nuclear particles in cancer treatment. Bristol: Adam Hilger Ltd.; 1981.

[15] Brahme A. Recent advances in light ion radiation therapy. Int J Radiat Oncol Biol Phys 2004;58:603–16.

[16] Lind BK, Brahme A. The radiation response of heterogeneous tumors. Phys Med 2007;23:91–9.

[17] Daşu A, Toma-Daşu I. Vascular oxygen content and the tissue oxygenation–a theoretical analysis. Med Phys 2008; 35:539–45.

[18] Krohn KA, Link JM, Mason RP. Molecular imaging of hypoxia. J Nucl Med 2008;49(Suppl 2):129S–148.

[19] Ling CC, Humm J, Larson S, Amols H, Fuks Z, Leibel S, et al. Towards multidimensional radiotherapy (MD-CRT): Biological imaging and biological conformality. Int J Radiat Oncol Biol Phys 2000;47:551–60.

[20] Tome WA, Fowler JF. On the inclusion of proliferation in tumour control probability calculations for inhomogeneously irradiated tumours. Phys Med Biol 2003;48:N261–8.

[21] Chao KSC, Bosch WR, Mutic S, Lewis JS, Dehdashti F, Mintun MA, et al. A novel approach to overcome hypoxic tumor resistance: Cu-ATSM-guided intensity-modulated radiation therapy. Int J Radiat Oncol Biol Phys 2001;49: 1171–82.

[22] Grosu AL, Souvatzoglou M, Roper B, Dobritz M, Wiedenmann N, Jacob V, et al. Hypoxia imaging with FAZA-PET and theoretical considerations with regard to dose painting for individualization of radiotherapy in patients with head and neck cancer. Int J Radiat Oncol Biol Phys 2007;69: 541–51.

[23] Lee ST, Scott AM. Hypoxia positron emission tomography imaging with 18f-fluoromisonidazole. Semin Nucl Med 2007;37:451–61.

[24] Xing L, Cotrutz C, Hunjan S, Boyer AL, Adalsteinsson E, Spielman D. Inverse planning for functional image-guided intensity-modulated radiation therapy. Phys Med Biol 2002; 47:3567–78.

[25] Alber M, Paulsen F, Eschmann SM, Machulla HJ. On biologically conformal boost dose optimization. Phys Med Biol 2003;48:N31–5.

[26] Das SK, Miften MM, Zhou S, Bell M, Munley MT, Whiddon CS, et al. Feasibility of optimizing the dose distribution in lung tumors using fluorine-18-fluorodeoxyglucose positron emission tomography and single photon emission computed tomography guided dose prescriptions. Med Phys 2004;31:1452–61.

[27] Malinen E, Sovik A, Hristov D, Bruland OS, Olsen DR. Adapting radiotherapy to hypoxic tumours. Phys Med Biol 2006;51:4903–21.

[28] Søvik A, Malinen E, Bruland OS, Bentzen SM, Olsen DR. Optimization of tumour control probability in hypoxic tumours by radiation dose redistribution: A modelling study. Phys Med Biol 2007;52:499–513.

[29] Flynn RT, Bowen SR, Bentzen SM, Rockwell MT, Jeraj R. Intensity-modulated x-ray (IMXT) versus proton (IMPT) therapy for theragnostic hypoxia-based dose painting. Phys Med Biol 2008;53:4153–67.

[30] Koh WJ, Bergman KS, Rasey JS, Peterson LM, Evans ML, Graham MM, et al. Evaluation of oxygenation status during fractionated radiotherapy in human nonsmall cell lung cancers using [F-18]fluoromisonidazole positron emission tomography. Int J Radiat Oncol Biol Phys 1995;33:391–8.

[31] Roels S, Slagmolen P, Nuyts J, Lee JA, Loeckx D, Maes F et al. Biological image-guided radiotherapy in rectal cancer: Is there a role for FMISO or FLT, next to FDG? Acta Oncol 2008;47:1237–48.

[32] Thorwarth D, Eschmann SM, Paulsen F, Alber M. Hypoxia dose painting by numbers: A planning study. Int J Radiat Oncol Biol Phys 2007;68:291–300.

[33] Brahme A. Biologically optimized 3-dimensional in vivo predictive assay-based radiation therapy using positron emission tomography-computerized tomography imaging. Acta Oncol 2003;42:123–36.

[34] Douglas BG, Fowler JF. Fractionation schedules and a quadratic dose-effect relationship. Br J Radiol 1975;48: 502–4.

[35] Barendsen GW. Dose fractionation, dose rate and iso-effect relationships for normal tissue responses. Int J Radiat Oncol Biol Phys 1982;8:1981–97.

[36] Fowler JF. The linear-quadratic formula and progress in fractionated radiotherapy. Br J Radiol 1989;62:679–94.

[37] Alper T, Howard-Flanders P. Role of oxygen in modifying the radiosensitivity of *E. Coli* B. Nature 1956;178:978–9.

[38] Alper T. Cellular radiobiology. Cambridge: Cambridge University Press; 1979.

[39] Thames HD, Bentzen SM, Turesson I, Overgaard M, Van den Bogaert W. Time-dose factors in radiotherapy: A review of the human data. Radiother Oncol 1990;19:219–35.
[40] Ågren Cronqvist AK, Kallman P, Turesson I, Brahme A. Volume and heterogeneity dependence of the dose-response relationship for head and neck tumours. Acta Oncol 1995; 34:851–60.
[41] Brahme A, Ågren AK. Optimal dose distribution for eradication of heterogeneous tumours. Acta Oncol 1987;26: 377–85.
[42] Ljungkvist ASE, Bussink J, Rijken PFJW, Kaanders JHAM, van der Kogel AJ, Denekamp J. Vascular architecture, hypoxia, and proliferation in first-generation xenografts of human head-and-neck squamous cell carcinomas. Int J Radiat Oncol Biol Phys 2002;54:215–28.
[43] Daşu A, Toma-Daşu I, Karlsson M. Theoretical simulation of tumour oxygenation and results from acute and chronic hypoxia. Phys Med Biol 2003;48:2829–42.
[44] Kelly CJ, Brady M. A model to simulate tumour oxygenation and dynamic [18F]-Fmiso PET data. Phys Med Biol 2006; 51:5859–73.
[45] Brahme A. Dosimetric precision requirements and quantities for characterizing the response of tumors and normal tissues. IAEA-TECDOC 1996;896:49–65.
[46] Brahme A. Dosimetric precision requirements in radiation therapy. Acta Radiol Oncol 1984;23:379–91.
[47] Vaupel P, Kallinowski F, Okunieff P. Blood flow, oxygen and nutrient supply, and metabolic microenvironment of human tumors: A review. Cancer Res 1989;49:6449–65.
[48] Daşu A, Toma-Daşu I. Theoretical simulation of tumour oxygenation – practical applications. Adv Exp Med Biol 2006;578:357–62.
[49] Toma-Daşu I, Daşu A, Brahme A. Quantifying tumour hypoxia by PET imaging – a theoretical analysis. Adv Exp Med Biol 2009;645:267–72.
[50] Gray LH, Conger AD, Ebert M, Hornsey S, Scott OCA. The concentration of oxygen dissolved in tissues at the time of irradiation as a factor in radiotherapy. Br J Radiol 1953; 26:638–48.
[51] Overgaard J. Hypoxic radiosensitization: Adored and ignored. J Clin Oncol 2007;25:4066–74.
[52] Chaplin DJ, Olive PL, Durand RE. Intermittent blood flow in a murine tumor: Radiobiological effects. Cancer Res 1987;47:597–601.
[53] Bussink J, Kaanders JHAM, Rijken PFJW, Peters JPW, Hodgkiss RJ, Marres HAM, et al. Vascular architecture and microenvironmental parameters in human squamous cell carcinoma xenografts: Effects of carbogen and nicotinamide. Radiother Oncol 1999;50:173–83.
[54] Rijken PFJW, Bernsen HJJA, Peters JPW, Hodgkiss RJ, Raleigh JA, van der Kogel AJ. Spatial relationship between hypoxia and the (perfused) vascular network in a human glioma xenograft: A quantitative multi-parameter analysis. Int J Radiat Oncol Biol Phys 2000;48:571–82.
[55] Eschmann SM, Paulsen F, Bedeshem C, Machulla HJ, Hehr T, Bamberg M, et al. Hypoxia-imaging with (18)F-Misonidazole and PET: Changes of kinetics during radiotherapy of head-and-neck cancer. Radiother Oncol 2007;83: 406–10.
[56] Chapman JD. The detection and measurement of hypoxic cells in solid tumors. Cancer 1984;54:2441–9.
[57] Toma-Daşu I, Uhrdin J, Daşu A, Brahme A. Therapy optimization based on non-linear uptake of PET tracers versus "linear dose painting". IFMBE Proceedings 2009 (in press).
[58] Lewis JS, McCarthy DW, McCarthy TJ, Fujibayashi Y, Welch MJ. Evaluation of 64Cu-ATSM in vitro and in vivo in a hypoxic tumor model. J Nucl Med 1999;40:177–83.
[59] Rasey JS, Hofstrand PD, Chin LK, Tewson TJ. Characterization of [18F]fluoroetanidazole, a new radiopharmaceutical for detecting tumor hypoxia. J Nucl Med 1999;40: 1072–9.
[60] Wijffels KI, Kaanders JH, Rijken PF, Bussink J, van den Hoogen FJ, Marres HA, et al. Vascular architecture and hypoxic profiles in human head and neck squamous cell carcinomas. Br J Cancer 2000;83:674–83.
[61] Gagel B, Reinartz P, Dimartino E, Zimny M, Pinkawa M, Maneschi P, et al. pO(2) Polarography versus positron emission tomography ([(18)F] fluoromisonidazole, [(18)F] -2-fluoro-2′-deoxyglucose). An appraisal of radiotherapeutically relevant hypoxia. Strahlenther Onkol 2004;180: 616–22.
[62] O'Donoghue JA, Zanzonico P, Pugachev A, Wen B, Smith-Jones P, Cai S, et al. Assessment of regional tumor hypoxia using 18F-fluoromisonidazole and 64Cu(II)-diacetyl-bis (N4-methylthiosemicarbazone) positron emission tomography: Comparative study featuring microPET imaging, Po2 probe measurement, autoradiography, and fluorescent microscopy in the R3327-AT and FaDu rat tumor models. Int J Radiat Oncol Biol Phys 2005;61:1493–502.
[63] Toma-Daşu I, Daşu A, Waites A, Denekamp J, Fowler JF. Theoretical simulation of oxygen tension measurement in the tissue using a microelectrode: II. Simulated measurements in tissues. Radiother Oncol 2002;64:109–18.
[64] Toma-Daşu I, Daşu A, Karlsson M. The relationship between temporal variation of hypoxia, polarographic measurements and predictions of tumour response to radiation. Phys Med Biol 2004;49:4463–75.
[65] Daşu A. Treatment planning optimisation based on imaging tumour proliferation and cell density. Acta Oncol 2008;47: 1221–8.